Journal of Molecular Structure 1108 (2016) 315–324

Contents lists available at ScienceDirect

Journal of Molecular Structure

journal homepage: http://www.elsevier.com/locate/molstruc

Synthesis, structure, photophysical and catalytic properties of Cu^I–Iodide complexes of di-imine ligands

Jahangir Mondal, Anupam Ghorai, Sunil K. Singh, Rajat Saha, Goutam K. Patra*

Department of Chemistry, Guru Ghasidas Vishwavidyalaya, Bilaspur, C.G, India

ARTICLE INFO

Article history:
Received 18 July 2015
Received in revised form
3 November 2015
Accepted 12 December 2015
Available online 17 December 2015

Keywords:
N-N donor ligand
$Cu^I I$ complexes
Crystal structure
Monomer
Dimer
Photophysics
Catalysis

ABSTRACT

Two new multifunctional $Cu^I I$ based complexes $[CuI(L^1)]$ **(1)** and $[Cu_2(\mu\text{-}I)_2(L^2)]$ **(2)** with bidentate N–N donor ligands $\mathbf{L^1}$ and imino-pyridyl ligand $\mathbf{L^2}$ have been synthesized and characterized by elemental analysis, IR, UV–Vis, NMR and single crystal X-ray crystallography. The bidentate di-imine ligand ($\mathbf{L^1}$) forms monomeric Cu^I complex (**1**) whereas the bis-bidentate di-imine ligand ($\mathbf{L^2}$) favours the formation of dimeric Cu^I complex (**2**) in association with two bridging iodides. Structural analysis reveals that in complex **1** each monomeric units are connected by $\pi\cdots\pi$ and C–H$\cdots\pi$ interactions to form 3D supramolecular structure whereas in complex **2** each molecules are connected by only $\pi\cdots\pi$ interactions to form 3D supramolecular structure. The photoluminescence properties of the complexes have been studied at room temperature. Theoretical analysis shows that HOMO is focused on the Cu and iodides while LUMO is focused on di-imine ligands and the luminescence behaviour arises due to metal to ligand charge transfer (MLCT) and halide to ligand charge transfer (XLCT). The complexes **1** and **2** are effective catalysts for the synthesis of 2-substituted benzoxazoles.

1. Introduction

Luminescent materials have attracted considerable attention for their numerous potential applications in solar energy conversion [1,2], luminescence-based sensors [3,4], organic light emitting diodes (OLEDs) [5–8] and biological labelling [9–11]. Monovalent group 11 metal ions, Au^I, Ag^I, and Cu^I, are well known for their interesting emissive properties [12]. Among these metal ions Cu^I is inexpensive and abundant and thus the synthesis and study of mono-/ploy-nuclear Cu^I complexes with di-imine ligands have become an important area of current research [13]. The judicious selection of N–N chelating ligands is the key point to control and tune the structure and luminescence properties [14–16]. The ancillary ligands such as halide and phosphine also have great effects on the emissive properties of the Cu^I-complexes [17–21]. Several excited states such as metal-centered transitions, intraligand transitions, and charge-transfer (CT) transitions between metal and ligands exist as emissive states, depending on the ligands and steric factors [22].

The largest class of luminescent Cu^I complexes has been investigated to date is that of $[Cu(N\text{–}N)_2]^+$, where N–N indicates a chelating ligand and the luminescence property of such complexes originates due to metal to ligand charge transfer (MLCT) [23–26]. In addition to the monomeric complexes, it has been noticed that the presence of halides favours the formation of polynuclear complexes with μ2-, μ3-, or μ4-bridging halide atoms, and their structures are also dependent on chelating ligand along with their synthetic procedure [27–31]. A number of complexes with a $\{Cu^I{}_2(\mu\text{-}I_2)\}$ unit have been prepared with various ligands and most of them possess a planar diamond core [32,33]. Studies on these complexes show that luminescence originates from $\{Cu^I{}_2(\mu\text{-}I_2)\}$ core to ligand charge transfer (MLCT) excited state, which is critical to the rigidity of the ligand.

In addition to this photophysical property, Cu(I) complexes are well-known for their catalytic properties. There are few examples in which Cu(I)-complexes act as efficient catalyst. G. Attilio Ardizzoia et al. have reported the catalytic cyclopropanation reactions of four Cu(I)-based complexes [34]. In another case, S. S. Chavan et al. have reported that the Cu(I)-complexes act as effective catalyst for the amination of aryl halides [35].

Herein, we have designed two different di-imine ligands; one is bidentate ($\mathbf{L^1}$) and the other is bis-bidentate ($\mathbf{L^2}$) and synthesized their Cu(I) complexes, **1** and **2** exploiting Cu(I)-iodides. Both the complexes are characterized by elemental analysis, IR, UV–Vis and

---

* Corresponding author.
E-mail address: patra29in@yahoo.co.in (G.K. Patra).

http://dx.doi.org/10.1016/j.molstruc.2015.12.028

single crystal X-ray crystallography. The bidentate ligand (**L^1**) forms the monomeric Cu^I complex (**1**) while the *bis*-bidentate ligand (**L^2**) favours the formation of dimeric complex (**2**) with very short Cu–Cu bond (2.486 Å) (Scheme 1). In complex **1**, metal ions shows trigonal geometry while in complex **2** each metal ions show tetrahedral geometry. In **2**, the dimer formation is favoured by μ-2 bridging of iodides. Supramolecular $\pi\cdots\pi$ and C–H$\cdots\pi$ interactions connect each monomeric units in **1** to form 3D supramolecular structure. And in **2**, each molecules are connected by supramolecular $\pi\cdots\pi$ interactions to form 3D supramolecular structure. The photoluminescence and catalytic properties of the complexes have been studied. However, as far we know, this is the first report of multifunctional properties of Cu(I)-complexes.

2. Experimental

2.1. Materials and measurements

All the reagents were procured commercially from Aldrich and used without further purification. Microanalyses were performed by Perkin–Elmer 2400II elemental analyzer. The melting point (mp) was determined by an electro-thermal IA9000 series digital melting point apparatus and is uncorrected. IR spectra (KBr disc) were recorded on a Nicolet Magna-IR spectrophotometer (Series II), UV–Vis spectra on a Shimadzu UV-160A spectrophotometer, ^{1}H and ^{13}C NMR spectra by a Brucker DPX200 spectrometer, EI mass spectra on a VG Autospec M–250 instrument. Photoluminescence spectra were recorded on a Perkin Elmer LS55 Luminescence Spectrometer.

2.2. Synthesis of ligands

2.2.1. Synthesis of ligand *L^1*

3.45 g (15 mmol) of 1- pyrenecarboxaldehyde was dissolved in 100 ml of anhydrous methanol. To this light yellowish solution 0.625 ml (7.5 mmol) of freshly distilled 1,2-diaminopropane was added drop-wise with stirring. Then, the reaction mixture was allowed to reflux for 6 h, maintaining dry conditions. The solvent was evaporated under reduced pressure to obtain a yellow solid. It was thoroughly washed with methanol. Yield: 2.615 g (70%); mp: 202–205 °C. Anal. calc. for $C_{37}H_{26}N_2$: C, 89.19 (89.13); H, 5.20 (5.25); N, 5.66 (5.62)%. EI-MS: 499.6 (M^+, 85%). FTIR/cm^{-1} (KBr): 1637(s), 1583(s), 843(vs), 829(m), 759(m), 716(vs), 682(m), 610(m). ^{1}H NMR (400 MHz, $CDCl_3$, TMS): δ 10.81 (d, 1H), 9.51 (s, 1H), 9.42 (s, 1H), 8.71 (dd, 2H), 8.52 (dd, 2H), 8.36 (m, 2H), 8.22 (m, 4H), 8.13 (m, 4H), 7.90 (m, 4H), 7.60 (dd, 2H), 1.65 (s, 3H, methyl protons). UV–VIS λ_{max}/nm (ε/dm^3 mol^{-1} cm^{-1}) (CH_3OH): 288 (27 500 260), 363 (10 250).

2.2.2. Synthesis of ligand *L^2*

2.36 g (15 mmol) of 2-quinolinecarboxaldehyde was dissolved in 100 ml of anhydrous methanol. To this yellowish solution 0.5 ml (7.5 mmol) of freshly distilled ethylene diamine was added dropwise with stirring. Then, the reaction mixture was allowed to reflux for 6 h, maintaining dry conditions. The solvent was evaporated under reduced pressure to obtain a yellow semi-solid, which on re-crystallization from diethyl ether gave yellow crystalline solid. Yield: 1.75 g (69%); mp: 128–130 °C. Anal. found (calc. for $C_{22}H_{18}N_4$): C, 77.65 (78.07); H, 5.37 (5.36); N, 16.65 (16.56)%. EI-MS: 338.1 (M^+, 84%); 181.1 ($M^+ - C_{10}H_6NO$, 25%); 169.1 ($M^+/2$, 98%). FTIR/cm^{-1} (KBr): 3451(vb), 3050 (m), 2890 (m), 1642(vs) (C=N), 1592(vs), 1557(s), 1500(vs), 1461(s), 1432(s), 1382(m), 1321(w), 1280(s), 1206(m), 1142 (m), 1108(s), 1030(s), 1015(w), 971(s), 941(m), 893(s), 868(s), 840(vs), 748(vs), 619(m), 492(m). ^{1}H NMR (200 MHz, $CDCl_3$, TMS): δ 8.63 (s, 2H), 8.17 (s, 4H), 8.11 (d, $J = 4$ Hz, 2H), 7.83–7.69 (m, 4H), 7.57 (t, $J = 4$ Hz, 2H), 4.18 (s, methylene, 4H). ^{13}C NMR (200 MHz, $CDCl_3$, TMS): δ 163.91, 154.52 (quaternary), 147.65 (quaternary), 136.50, 129.70, 129.50, 128.71 (quaternary), 127.63, 127.34, 118.40, 61.43. UV–VIS λ_{max}/nm (ε/dm^3 mol^{-1} cm^{-1}) (CH_3OH): 290 (10 260), 242 (42 710).

2.3. Preparation of complexes

2.3.1. Synthesis of [CuI(L^1)] **(1)**

CuI (0.19 g, 1 mmol) dissolved in acetonitrile (30 ml) is added dropwise into a 20 ml chloroform solution of the ligand L^1 (0.498 g, 1 mmol) within 1 h. Then the brownish reaction mixture is stirred for another 1 h at room temperature. Reddish brown complex has appeared. It is filtered out and washed with 5 ml acetonitrile and dried *in vacuo*; yield, 4.485 g (65%). Deep red single crystals suitable for X-ray analysis are obtained by careful layering of CuI (1.9 mg, 0.01 mmol) dissolved in acetonitrile (4 ml) onto a 4 ml chloroform solution of the ligand L^1 (5 mg, 0.01 mmol). Anal. Calcd. for $C_{37}H_{26}N_2CuI$: C 64.49, H 3.80, N 4.06; found: C 64.43, H 3.87, N 4.10. FTIR cm^{-1} (KBr): 3047(m), 2922(m), 1613(s), 1593(s), 1252(m), 1234(s), 1108(m), 994(m), 844(vs), 824(m), 767(s), 715(vs), 475(m). UV–Vis (MeCN) [$\lambda_{max,}$ nm]: 283, 366.

2.3.2. Synthesis of [$Cu_2(\mu$-$I)_2(L^2)$] **(2)**

CuI (0.19 g, 1 mmol) dissolved in acetonitrile (30 ml) is added dropwise into a 20 ml chloroform solution of the ligand L^2 (0.338 g, 1 mmol) within 1 h. Then the reddish reaction mixture is stirred for

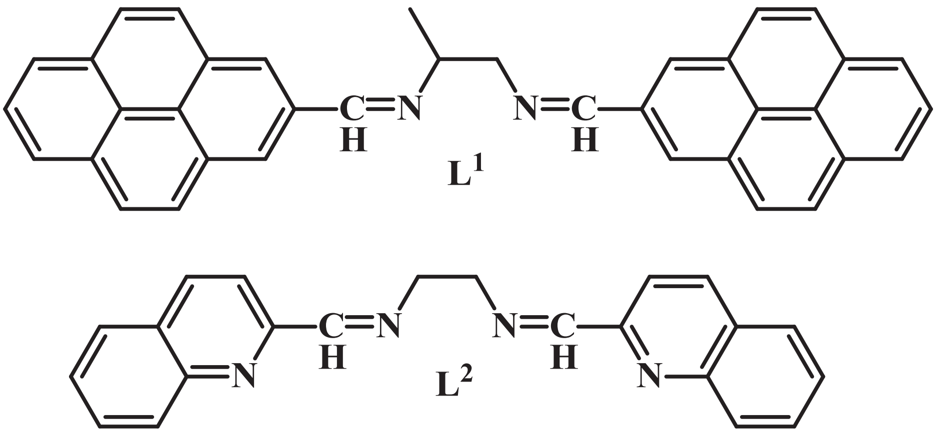

Scheme 1. Chemical structure of the ligands **L^1** and **L^2** used in this study.

another 1 h at room temperature. Deep red colored solid precipitated out. It was filtered out and washed with 5 ml acetonitrile and dried *in vacuo*. Yield: 5.177 g (72%). Deep red single crystals suitable for X-ray analysis are obtained by careful layering of CuI (3.8 mg, 0.02 mmol) dissolved in acetonitrile (4 ml) onto a 4 ml chloroform solution of the ligand L^2 (6.8 mg, 0.02 mmol). Anal. Calcd for $C_{22}H_{18}N_4Cu_2I_2$: C 36.73, H 2.52, N 7.79; found: C 36.80, H 2.54, N 7.83. FTIR cm^{-1} (KBr): 3047(m), 2922(m), 1613(s), 1573(m), 1252(m), 1234(s), 1108(m), 994(m), 844(vs), 824(m), 767(s), 720(vs), 475(m),. UV–Vis (MeCN) [$\lambda_{max,}$ nm]: 530, 350, 290.

2.4. Crystallographic data collection and refinement

Suitable single crystals of the complexes were mounted on a Bruker SMART diffractometer equipped with a graphite monochromator and Mo-K_α (λ = 0.71073 Å) radiation. The structures were solved using Patterson method by using the SHELXS97. Subsequent difference Fourier synthesis and least-square refinement revealed the positions of the remaining non hydrogen atoms. Non-hydrogen atoms were refined with independent anisotropic displacement parameters. Hydrogen atoms were placed in idealized positions and their displacement parameters were fixed to be 1.2 times larger than those of the attached non-hydrogen atom. Successful convergence was indicated by the maximum shift/error of 0.001 for the last cycle of the least squares refinement. All calculations were carried out using SHELXS 97 [36], SHELXL 97 [37], PLATON 99 [38], ORTEP-32 [39] and WinGX system Ver-1.64 [40]. Data collection and structure refinement parameters and crystallographic data for the complexes are given in Table 1. Selected coordination bond lengths, bond angles and non-covalent interaction parameters are summarized in Tables 2–5.

2.5. Computational details

The GAUSSIAN-09 Revision C.01 program package was used for all calculations [41]. The gas phase geometries of the compounds were fully optimized without any symmetry restrictions in singlet ground state with the hybrid B3LYP [42,43] exchange-correlation functional. Frequency calculations while optimizations of the structures have no non-negative frequency, which implies that, the structures obtained having true minima. Basis set 6–31++G was found to be suitable for the whole molecule.

3. Result and discussions

3.1. Synthetic aspects

The Schiff-base ligand $\mathbf{L^1}$ was prepared in good yield by the condensation of 1, 2-diaminopropane with 1-pyrinealdehyde in 1:2 M ratio in dry methanol maintaining dry condition throughout the reaction. Reaction of CuI and diimine ligand $\mathbf{L^1}$ in 1:1 mol ratio in room temperature yielded the brown red-coloured mono-nuclear complex **1**. Ligand $\mathbf{L^2}$ is 1:2 condensate of ethylene diamine and quinolone-2-carboxaldehyde. The ligand $\mathbf{L^1}$ contains two and ligand $\mathbf{L^2}$ contains four N-sites suitable to coordinate to the metal ions, and are conformationally flexible about the central saturated

Table 1
Summary of crystallographic data for complexes **1** and **2**.

	Complex 1	Complex 2
Formula	$C_{37}H_{26}CuIN_2$	$C_{22}H_{18}Cu_2I_2N_4$
Formula Weight	689.04	719.30
Crystal System	Monoclinic	Monoclinic
Space group	$P2_1$/c (No. 14)	$P2_1$/n (No. 14)
a [Å]	15.765(3)	9.1190(6)
b [Å]	8.9392(17)	17.2073(12)
c [Å]	21.219(4)	14.4576(10)
β [°]	108.696(4)	96.996(1)
V [$Å^3$]	2832.5(9)	2251.7(3)
Z	4	4
D(calc) [g/cm^3]	1.616	2.122
μ(MoKα) [/mm]	1.891	4.648
F(000)	1376	1368
Crystal Size [mm]	0.08 × 0.10 × 0.12	0.06 × 0.08 x 0.10
Temperature (K)	293	293
Radiation [Å]	MoKα 0.71073	MoKα 0.71073
θ Min-Max [°]	1.4; 25.3	1.9; 28.8
Dataset	−18: 18; −10: 10; −25: 25	−12: 11; −22: 22; −18: 18
Total & Uniq. Data	26344; 5114	24071, 5575
R(int)	0.044	0.039
Observed data [I > 2.0 σ(I)]	3819	4561
Nref, Npar	5114, 371	5575, 271
R	0.0529	0.0261
wR2	0.1420	0.0643
S	1.07	0.81
Max. and Av. Shift/Error	0.00, 0.00	0.00, 0.00
Min. & Max. Resd. Dens. [e/$Å^3$]	−1.54; 1.18	−0.53, 0.69

w = 1/[\sˆ2ˆ(Foˆ2ˆ)+(0.0545P)ˆ2ˆ+7.0650P] where P=(Foˆ2ˆ+2Fcˆ2ˆ)/3.

Table 2
Some selected coordination bond distances (Å) and bond angles (°) of complex **1**.

	Experimental	Theoretical		Experimental	Theoretical
I1–Cu2	2.4177(12)	2.44	Cu2–N1	2.047(8)	2.03
Cu2–N2	2.050(6)	2.03	I1–Cu2–N1	135.4(2)	134.6
I1–Cu2–N2	138.81(17)	137.6	N1–Cu2–N2	84.0(3)	85.3

Table 3
All the π··· interaction parameters of complex **1**.

Π···π interactions			
Ri···Rj	Distance between ring Centroids (Å)	Dihedral Angle between Planes I and J (°)	Symmetry
R3···R5	3.706(4)	2.3(3)	1-x, -y, 1-z
R4···R5	3.717(3)	1.9(3)	1-x, -y, 1-z
R5···R3	3.705(4)	2.3(3)	1-x, -y, 1-z
R5···R4	3.717(3)	1.9(3)	1-x, -y, 1-z
R5···R5	3.634(3)	0	1-x, -y, 1-z
R6···R6	3.636(5)	0	-x, -y, -z
R6···R8	3.984(4)	1.9(4)	-x, -y, -z
R8···R6	3.984(4)	1.9(4)	-x, -y, -z
C–H···π interactions			
C–H···Ri	H···Ri (Å)	<C–H···Ri (°)	Symmetry
C2–H2···R9	2.66	153	1-x, −1/2 + y, 1/2-z
C36–H36A···R5	2.66	153	1-x, −1/2 + y, 1/2-z

*R3: C1- > C14- > C13- > C12- > C15- > C16->; R4: C5- > C6- > C7- > C8- > C15- > C16->; R5: C8- > C9- > C10- > C11- > C12- > C15->; R6: C19- > C20- > C21- > C31- > C22- > C27->; R7: C19- > C27- > C26- > C30- > C34- > C33->; R8: C22- > C23- > C24- > C25- > C26- > C27->; R9: C25- > C26- > C30- > C29- > C35- > C28->

C–C bond. In the presence of suitable metal ions, **L^1** and **L^2** can adopt readily a different conformation about this bond in order to arrange the nitrogen binding sites in a convergent manner and optimize the metal-ligand coordination. The bright red homo-dinuclear complex **2** is synthesised by the reaction of CuI with the ligand **L^2** in 1:1 mol ratio at room temperature. Synthetic procedure for complex **2** is given in Scheme 2. The complexes are air-stable in solid state for at least 10 weeks. The solubility of the complex **1** is better than the complex **2** in common solvents like acetonitrile, dimethyl formamide and dimethyl sulphoxide. The stability of the dissolved complexes **1** and **2** in air is one-week.

3.2. *Description of crystal structures*

3.2.1. *Molecular and supramolecular structure of* ***1***

Single crystal X-ray diffraction analysis reveals that complex **1** is

Table 4
Some selected coordination bond distances (Å) and bond angles (°) of complex **2**.

	Experimental	Theoretical		Experimental	Theoretical
I1–Cu3	2.6513(5)	2.64	I1–Cu4	2.5948(4)	2.61
I2–Cu3	2.6078(5)	2.62	I2–Cu4	2.6680(5)	2.64
Cu3–N1	2.034(3)	2.02	Cu3–N2	2.102(3)	2.11
Cu4–N3	2.093(3)	2.07	Cu4–N4	2.035(2)	2.04
I1–Cu3–I2	107.22(1)	106.1	I1–Cu3–N1	115.46(7)	116.3
I1–Cu3–N2	122.49(7)	121.3	I2–Cu3–N1	122.88(7)	121.1
I2–Cu3–N2	106.80(7)	104.8	N1–Cu3–N2	80.69(10)	79.6
I1–Cu4–I2	107.10(1)	105.5	I1–Cu4–N3	116.95(7)	114.8
I1–Cu4–N4	124.84(7)	123.6	I2–Cu4–N3	113.99(7)	110.7
I2–Cu4–N4	111.70(7)	110.2	N3–Cu4–N4	80.54(10)	78.9

Table 5
All the π··· interaction parameters of complex **2**.

π···π interactions			
Ri···Rj	Distance between ring centroids (Å)	Dihedral angle between planes I and J (°)	Symmetry
R4···R4	3.7101(16)	0	1-x, −y, 1-z
R4···R5	3.6736(16)	16.24(13)	3/2-x, −1/2 + y, 1/2-z
R4···R6	3.7186(17)	2.37(14)	1-x, −y, 1-z
R5···R4	3.6736(16)	16.24(13)	3/2-x, 1/2 + y, 1/2-z
R5···R5	3.6916(16)	0	2-x, 1-y, 1-z
R5···R7	3.5827(16)	3.33(13)	2-x, 1-y, 1-z
R6···R4	3.7186(17)	2.37(14)	1-x, −y, 1-z
R7···R5	3.5828(16)	3.33(13)	2-x, 1-y, 1-z

*R4: N1- > C2- > C1- > C18- > C4- > C3->; R5: N4- > C8- > C9- > C10- > C11- > C12->; R6: C3- > C4- > C19- > C20- > C21- > C22->; R7: C11- > C12- > C13- > C14- > C15- > C16->

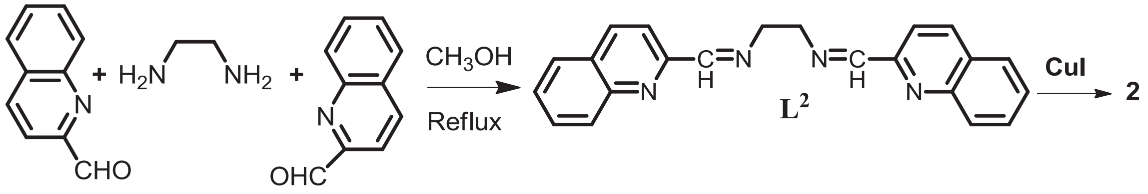

Scheme 2. Synthetic route of the ligand **L^2** and the complex **2**.

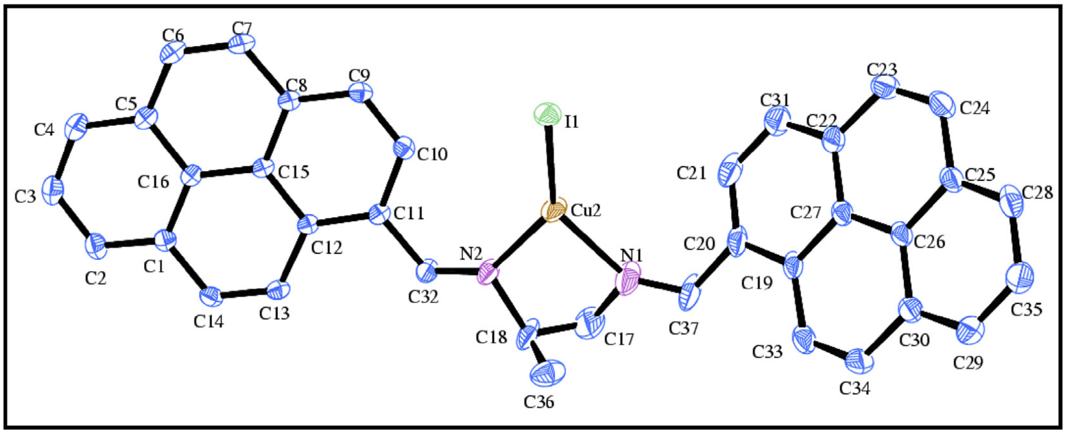

Fig. 1. ORTEP diagram of complex **1**.

a monomeric metal-organic structure of Cu(I) and crystallizes in achiral $P2_1/c$ space group. Each asymmetric unit contains one Cu^+ ion, one neutral bidentate ligand (**L^1**) and one coordinating iodide ion (I^-). The ORTEP diagram of the asymmetric unit is shown in Fig. 1. Some selected bond lengths and bond angles are given in Table 2. Each Cu atom is tri-coordinated (N1, N2 and I1) and shows almost triangular planar geometry. For the Cu2 atom, N1 and N2 atoms of the ligand (**L^1**) and the one iodide form the coordination sphere. The Cu—N bond distances vary in the range of 2.047(8) – 2.050(6) Å and Cu—I bond distance is 2.4177(12) Å.

Supramolecular $\pi\cdots\pi$ interactions connect the monomeric units to form 2D supramolecular layer structure, as shown in Fig. 2. C—H$\cdots\pi$ interactions bridge these 2D supramolecular polymers to form 3D supramolecular framework in Fig. 3. All the $\pi\cdots$ interactions are summarized in Table 3.

3.2.2. *Molecular and supramolecular structure of complex **2***

Single crystal X-ray diffraction analysis reveals that complex **2** is a di-meric 0D metal-organic structure of Cu(I) and crystallizes in achiral $P2_1/n$ space group. Each asymmetric unit contains two Cu^+ ions, one neutral tetra-dentate ligand (**L^2**) and two bridging iodide ions (I^-). The ORTEP diagram of the asymmetric unit is shown in Fig. 4. Two Cu^I ions are bridged by two iodides with formation of $\{Cu^I_2I_2\}$ unit and one *bis*-bidentate ligand (**L^2**). Some selected bond lengths and bond angles are given in Table 4. Each Cu atom is four coordinated with distorted tetrahedral geometry. For the Cu3 atom, N1 and N2 atoms of the ligand (**L^2**) and the two iodides (I1 and I2) form the coordination sphere while for Cu4 atom N3 and N4 atoms of the ligand (**L^2**) and the same two iodides (I1 and I2) are at the coordination sphere. The Cu—N bond distances vary in the range of 2.034(3)-2.102(3) Å and Cu—I bond distances vary in the range of 2.5948(4) - 2.6680(5) Å. The *bis*-bidentate di-imine ligand (**L^2**) binds two metal centres and the two iodides act as a μ-2-bridging ligand. The Cu—Cu distance within this dimeric complex is 2.486 Å, which is comparable with those found in other copper(I) dimeric complexes.

Supramolecular $\pi\cdots\pi$ interactions connect the monomeric units to form 3D supramolecular structure, Fig. 5. All the $\pi\cdots$ interactions

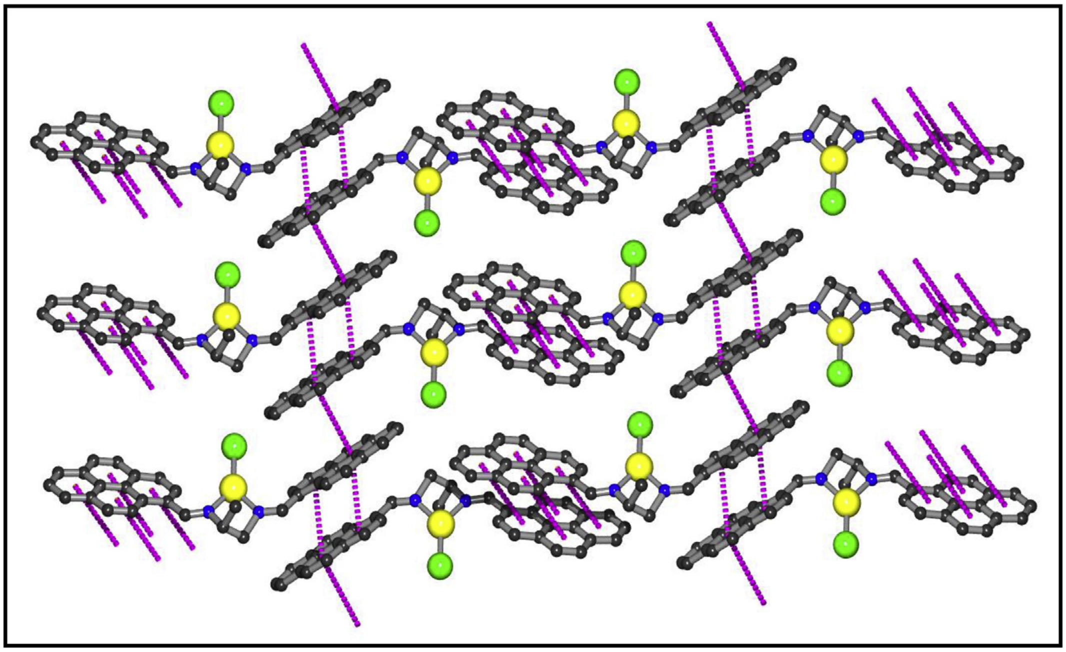

Fig. 2. 2D supramolecular sheet structure formed by $\pi\cdots\pi$ interactions of complex **1**.

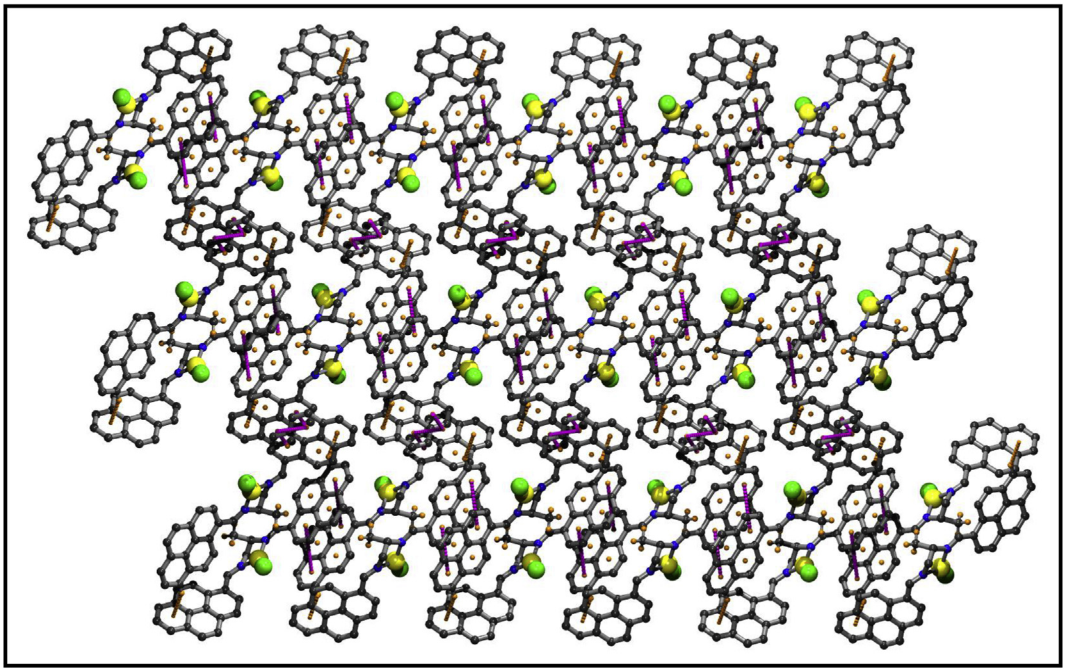

Fig. 3. 3D supramolecular structure formed by both $\pi \cdots \pi$ and C–H$\cdots\pi$ interactions in complex **1**.

are summarized in Table 5.

3.2.3. Comparison between the calculated and experimental data

We have compared our calculated bond distances and bond angles of complexes **1** and **2**, with those obtained from X-ray single crystal data. These data have been tabulated in Tables 2 and 4. From the comparison it is clear that calculated bond distances and bond angles of complexes **1** and **2** are in good agreement with the experimental data. The difference for particular bond using experimental and calculated value lies within 0.028Å–0.01 Å and difference in bond angle lies within 1°–3.2°.

3.3. IR spectroscopy

The complexation processes of the ligands have been monitored by IR spectroscopy. The IR spectrum of the ligand $\mathbf{L^1}$ and $\mathbf{L^2}$ show characteristic bands at, 1637 and 1583 cm^{-1} (for $\mathbf{L^1}$) and 1642 and 1600 cm^{-1} (for $\mathbf{L^2}$) which we assign to the pyridine/quinoline ring and imine C=N stretching frequencies respectively. For the Cu(I) complexes these bands appear at 1613 and 1599 cm^{-1} (for **1**); 1613 and 1573 cm^{-1} (for **2**). The IR stretching frequency of CH_3 group of the ligand $\mathbf{L^2}$ appears at 715 cm^{-1} and that of the complex **2** appears at 720 cm^{-1}.

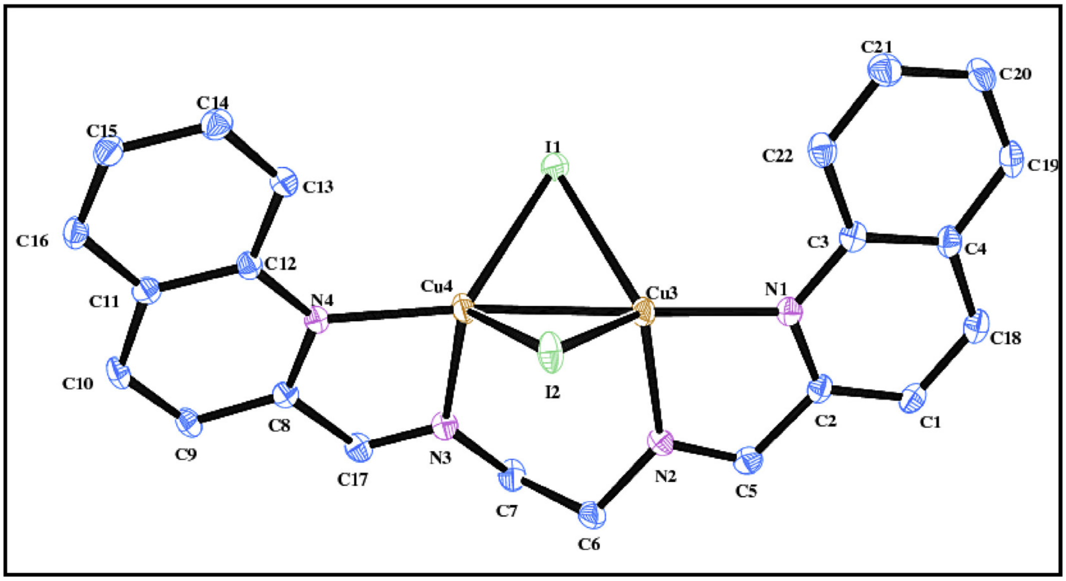

Fig. 4. ORTEP diagram of complex **2**.

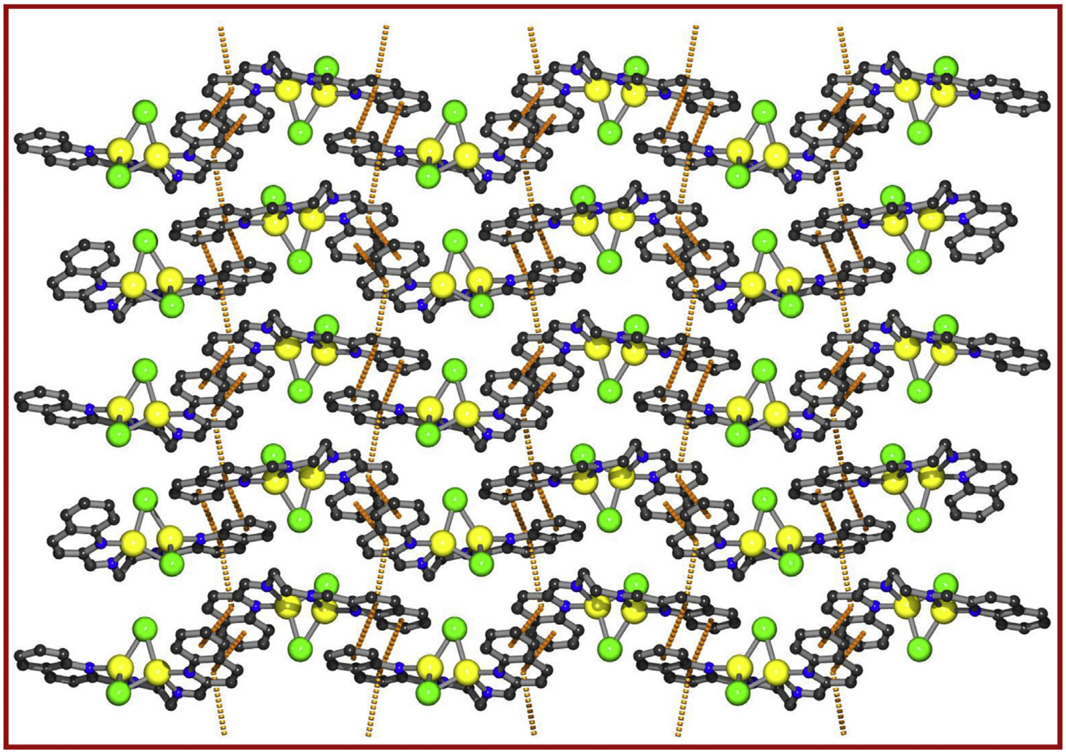

Fig. 5. 3D supramolecular structure of the complex **2**.

3.4. Photoluminescence properties

The emission spectra of both complexes were studied in solid state at room temperature. The complex **1** shows emission maxima at ca. 435 nm with shoulder at ca. 481 nm (Fig. 6) upon excitation at 290 nm. The complex **2** shows emission maxima at ca. 422 nm with shoulders at ca. 398 nm and ca. 460 nm (Fig. 7) upon excitation at 290 nm. To gain insight into the photophysical properties of the complexes, we have optimized the structures at ground state of these complexes, using DFT method. This calculations may be instructive to analyze the highest occupied molecular orbital (HOMO) and lowest unoccupied molecular orbital (LUMO) of the complexes (Fig. 8). Theoretical analysis reveals that HOMOs are focused on the Cu and Iodide and the LUMOs are focused on di-imine ligands.

So, it can be concluded that for complex **1** the emission spectra is produced due to charge transfer from Cu—I core to the bidentate ligand and for complex **2** the emission spectra is produced due to charge transfer from the $\{Cu_2(\mu\text{-}I)_2\}$ core to the *bis*-bidentate ligand, similar to the complexes with $\{Cu_2X_2\}$ diamond cores with di-imine ligands.

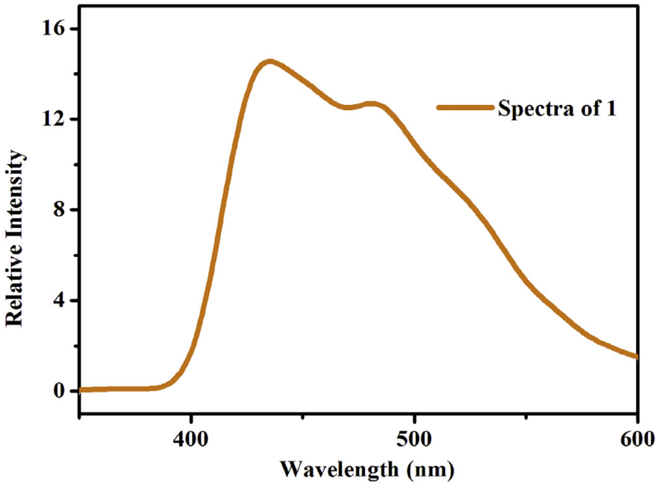

Fig. 6. Photoluminescence spectra of complex **1**.

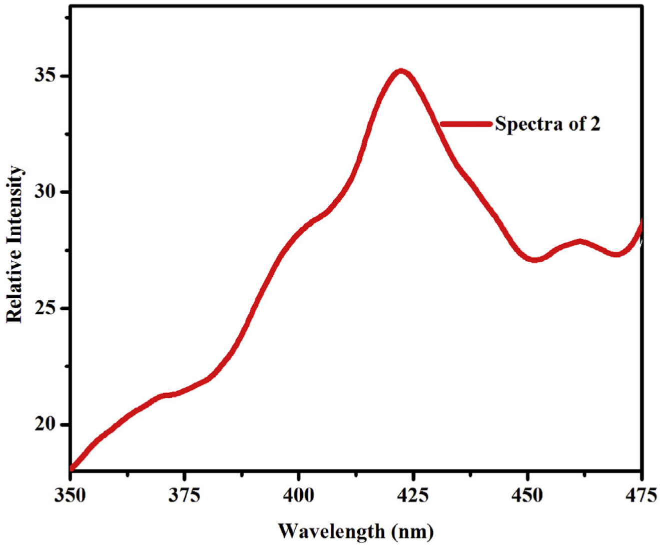

Fig. 7. Photoluminescence spectra of complex **2**.

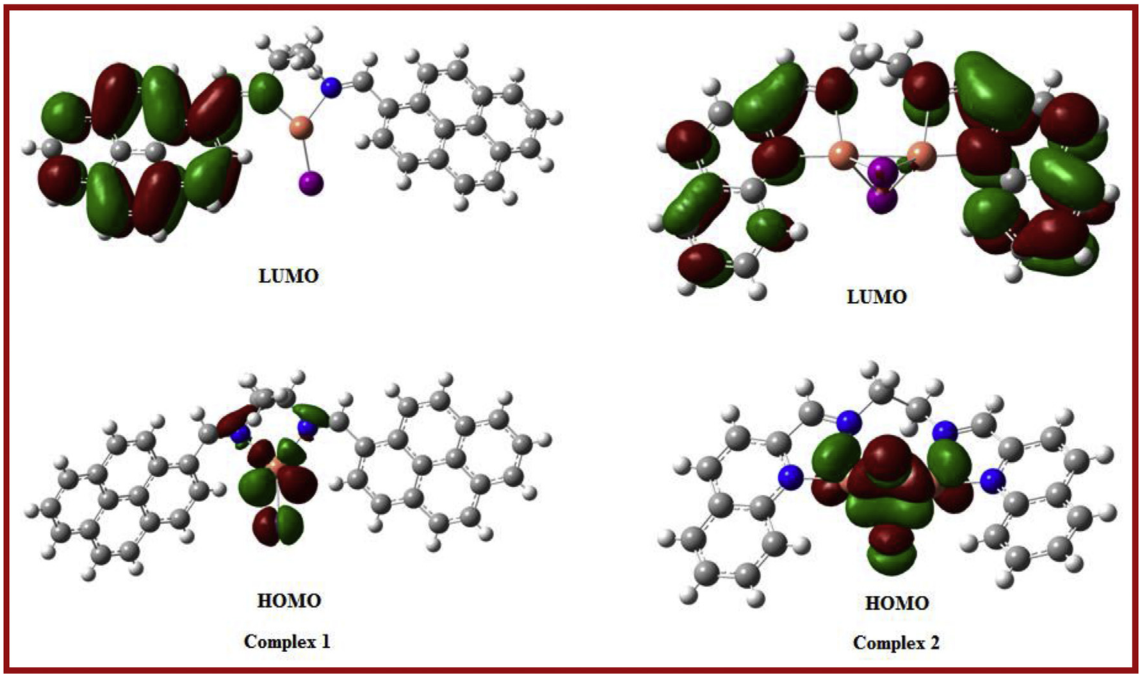

Fig. 8. HOMO and LUMO of the complexes **1** and **2**.

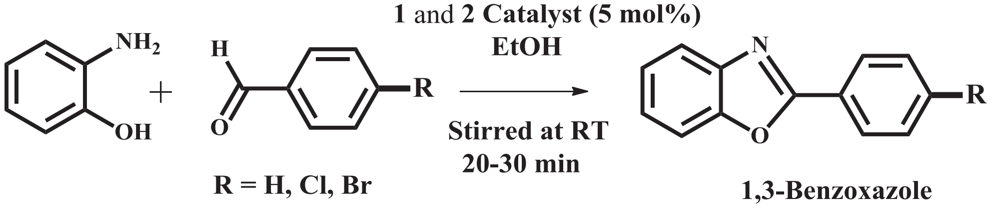

Scheme 3. **1** and **2** catalysed synthesis of 1,3-Benzoxazole.

Table 6
Synthesis of 2-aryl 1,3-benzoxazole.

Entry	Ar-CHO	Time (min)	Product	Complex	Yield (%)	Melting point °C		Ref.
						Observed	Reported	
1.		21	**1a**	1 2	48 52	110–113	112–114	54
2.	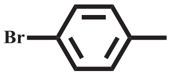	19	**1b**	1 2	62 63	129–131	130–131	55
3.		16	**1c**	1 2	69 69	113–116	114–116	54
4.	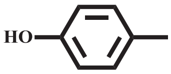	22	**1d**	1 2	73 76	285–287	287–289	56
5.		25	**1e**	1 2	65 64	103–106	102–104	54

3.5. Catalytic activity

Cu(I)-complexes-catalyzed cyclopropanation of alkenes has attracted enormous research interest. Benzoxazoles are a class of heterocycles with a diverse spectrum of biological properties [44]. More particularly, 2-substituted benzoxazoles are of great interest owing to their potent utility as antirheumatic agent [45], H37Rv inhibitor [46], elastase inhibitor [47,48] HT3 receptor agonist [49], cytotoxic compound toward P338 cell [50] and chemiluminescent agents [51]. Moreover, benzoxazoles derivatives are isosteres of naturally occurring cyclic nucleotides and they interact with the biopolymers of organisms [52]. This broad utility has prompted significant efforts toward the synthesis of these heterocycles [47–58]. Herein, we are reporting the catalytic activity of the two copper (I) complexes **1** and **2** in the synthesis of 2-substitued 1,3-benzoxazoles (**1a**, **1b**, **1c, 1d** and **1e**).

Complexes **1** and **2** have been proved to be excellent catalyst for the condensation of benzaldehyde and its -bromo, -chloro, -hydroxy and -methoxy derivatives with o-aminophenol. The effect of **1** and **2** as catalysts for the synthesis of 2-phenyl-1,3-benzoxazoles was investigated and the complexes have been found promising in affording the corresponding benzoxazoles in moderate to good yields. In this protocol we report the catalytic efficiency of these complexes under mild and environmental friendly conditions and thus all the reactions were carried out at room temperature using ethanol (a non-toxic solvent) (Scheme 3). It was observed that no further increase in the yield of the product occurred even when the reaction time was increased (4 h). Dinuclear complex **2** shows greater activity than the mononuclear complex **1** and the percentage of yield for complex **2** reached up to 52–76% (Table 6). These results could be attributed to the presence of two self-repeating units in complex **2**. Blank experiments have also been performed without catalyst and with CuI. In presence of CuI, the reaction rate was very slow; after 10 h only 10–18% of benzaldehyde was converted into products. In absence of both CuI and catalyst, the reactants can't form the products.

The reaction in general is simple enough as the solid products were purified by recrystallization from ethanol. Tedious purification by column chromatography was thus avoided in this protocol. The pure isolated products were then characterized by their melting points which were consistent with those described in the literature (the corresponding references were given in Table 6). Further these compounds were characterized by UV–Vis and NMR spectroscopy.

4. Conclusions

In summary, we have successfully presented the multifunctional properties of two new Cu^I–I complexes for the first time. The complexes have been synthesized using two different ligands: bidentate ligand $\mathbf{L^1}$ and tetradentate ligand $\mathbf{L^2}$. $\mathbf{L^1}$ forms only monomeric complex (**1**) whereas the *bis*-bidentate di-imine ligand $\mathbf{L^2}$ favours the formation of dimeric complex (**2**) in association with two bridging iodides. In complex **1** each monomeric units are connected by $\pi\cdots\pi$ and C–H$\cdots\pi$ interactions to form 3D supramolecular structure whereas in complex **2**, each molecules are connected by only $\pi\cdots\pi$ interactions to form 3D supramolecular structure. Theoretical analysis shows that the HOMO is focused on the Cu and Iodides while LUMO is focused on di-imine ligands and the luminescence behaviour arises due to metal to ligand charge transfer (MLCT) and halide to ligand charge transfer (XLCT). The complexes **1** and **2** are effective catalysts for synthesis of 2-substituted 1, 3-benzoxazoles.

Acknowledgements

G.K.P would like to thank the Department of Science and Technology and Department of Biotechnology, Government of India, New Delhi for financial support.

Appendix A. Supplementary data

CCDC reference numbers of the complexes **1** and **2** are **1405108** and **1405109** respectively. These data can be obtained free of charge via http://www.ccdc.cam.ac.uk/conts/retrieving.html.

References

[1] S. Hattori, Y. Wada, S. Yanagida, S. Fukuzumi, J. Am. Chem. Soc. 127 (2005) 9648.

[2] F. Franceschi, M. Guardigli, E. Solari, C. Floriani, A. ChiesiVilla, C. Rizzoli, Inorg. Chem. 36 (1997) 4099.

[3] C.S. Smith, K.R. Mann, Chem. Mater 21 (2009) 5042.

[4] L.N. Sun, J.B. Yu, H.S. Peng, J.Z. Zhang, L.Y. Shi, O.S. Wolfbeis, J. Phys. Chem. C 114 (2010) 12642.

[5] Z.S. Su, G.B. Che, W.L. Li, W.M. Su, M.T. Li, B. Chu, B. Li, Z.Q. Zhang, Z.Z. Hu, Appl. Phys. Lett. 88 (2006) 213508.

[6] Y.M. Wang, F. Teng, Y.B. Hou, Z. Xu, Y.S. Wang, W.F. Fu, Appl. Phys. Lett. 87 (2005) 233512.

[7] Y.G. Ma, C.M. Che, H.Y. Chao, X.M. Zhou, W.H. Chan, J.C. Shen, Adv. Mater 11 (1999) 852.

[8] A. Tsuboyama, K. Kuge, M. Furugori, S. Okada, M. Hoshino, K. Ueno, Inorg. Chem. 46 (2007) 1992.

[9] M.H. Lim, D. Xu, S.J. Lippard, Nat. Chem. Biol. 2 (2006) 375.

[10] Z.W. Wei, L.N. Sun, J.L. Liu, J.Z. Zhang, H.R. Yang, Y. Yang, L.Y. Shi, Biomaterials 35 (2014) 387.

[11] Z. Liu, L.N. Sun, F.Y. Li, Q. Liu, L.Y. Shi, D.S. Zhang, S. Yuan, T. Liu, Y.N. Qiu, J. Mater. Chem. 21 (2011) 17615.

[12] (a) P.C. Ford, E. Cariati, J. Bourassa, Chem. Rev. 99 (1999) 3625;
(b) A. Vogler, H. Kunkely, Coord. Chem. Rev. 489 (2001) 219;
(c) R.L. White-Morris, M.M. Olmstead, A.L. Balch, J. Am. Chem. Soc. 125 (2003) 1033;
(d) V.W.-W. Yam, K.K.-W. Lo, Chem. Soc. Rev. 28 (1999) 323;
(e) D.R. McMillin, K.M. McNett, Chem. Rev. 98 (1998) 1201;
(f) N. Armaroli, Chem. Soc. Rev. 30 (2001) 113;
(g) C.-M. Che, Z. Mao, V.M. Miskowski, M.-C. Tse, C.-K. Chan, K.-K. Cheung, D.L. Phillips, K.-H. Leung, Angew. Chem. Int. Ed. 39 (2000) 4084.

[13] F. Wei, X. Liu, Z. Liu, Z. Bian, Y. Zhao, C. Huanga, Cryst. Eng. Comm. 16 (2014) 5338.

[14] N. Armaroli, G. Accorsi, M. Holler, O. Moudam, J.-F. Nierengarten, Z. Zhou, R.T. Wegh, R. Welter, Adv. Mater. 18 (2006) 1313.

[15] Q. Zhang, Q. Zhou, Y. Cheng, L. Wang, D. Ma, X. Jing, F. Wang, Adv. Mater. 16 (2004) 432.

[16] M. Nishikawa, K. Nomoto, S. Kume, K. Inoue, M. Sakai, M. Fujii, H. Nishihara, J. Am. Chem. Soc. 132 (2010) 9579.

[17] T. McCormick, W.-L. Jia, S. Wang, Inorg. Chem. 45 (2006) 147.

[18] D.G. Cuttell, S.M. Kuang, P.E. Fanwick, D.R. McMillin, R.A. Walton, J. Am. Chem. Soc. 124 (2002) 6.

[19] C.S. Smith, C.W. Branham, B.J. Marquardt, K.R. Mann, J. Am. Chem. Soc. 132 (2010) 14079.

[20] C.K. Ryu, M. Vitale, P.C. Ford, Inorg. Chem. 32 (1993) 869.

[21] A. Tsuboyama, K. Kuge, M. Furugori, S. Okada, M. Hoshino, K. Ueno, Inorg. Chem. 46 (2007) 1992.

[22] P.C. Ford, E. Cariati, J. Bourassa, Chem. Rev. 99 (1999) 3625.

[23] N. Armaroli, Chem. Soc. Rev. 30 (2001) 113.

[24] D.V. Scaltrito, D.W. Thompson, J.A. O'Callaghan, G.J. Meyer, Coord. Chem. Rev. 208 (2000) 243.

[25] N. Armaroli, G. Accorsi, F. Cardinali, A. Listorti, Top. Curr. Chem. 280 (2007) 69.

[26] A. Barbieri, G. Accorsi, N. Armaroli, Chem. Commun. (2008) 2185.

[27] M. Vitale, P.C. Ford, Coord. Chem. Rev. 3 (2001) 219.

[28] W.H. Chan, Z.Z. Zhang, T.C.W. Mak, C.M. Che, J. Organomet. Chem. 556 (1998) 169.

[29] R. Provencher, P.D. Harvey, Inorg. Chem. 35 (1996) 2235.

[30] V.W.W. Yam, K.K.W. Lo, K.K. Cheung, Inorg. Chem. 35 (1996) 3459.

[31] K.R. Kyle, C.K. Ryu, J.A. Dibenedetto, P.C. Ford, J. Am. Chem. Soc. 113 (1991) 2954.

[32] H. Araki, K. Tsuge, Y. Sasaki, S. Ishizaka, N. Kitamura, Inorg. Chem. 44 (2005) 9667.

[33] (a) J.T. Maeyer, T.J. Johnson, A.K. Smith, B.D. Borne, R.D. Pike, W.T. Pennington, M. Krawiec, A.L. Rheingold, Polyhedron 22 (2003) 419;
(b) P.M. Graham, R.D. Pike, M. Sabat, R.D. Bailey, W.T. Pennington, Inorg. Chem. 39 (2000) 5121;
(c) G.A. Bowmaker, R.D. Hart, B.E. Jones, B.W. Skelton, A.H. White, J. Chem. Soc. Dalton Trans. (1995) 3063;
(d) G.A. Bowmaker, J.V. Hanna, R.D. Hart, P.C. Healy, A.H. White, Aust. J. Chem. 47 (1994) 25.

[34] G.A. Ardizzoia, S. Brenna, F. Castelli, S. Galli, Inorg. Chim. Acta 362 (2009) 3507.

[35] S.S. Chavan, S.K. Sawant, V.A. Sawant, G.K. Lahiri, Inorg. Chem. Comm. 14 (2011) 1373.

[36] G.M. Sheldrick, SHELXS 97, Program for Structure Solution, University of Gottingen, Germany, 1997.

[37] G.M. Sheldrick, SHELXL 97, Program for Crystal Structure Refinement, University of Gottingen, Germany, 1997.

[38] A.L. Spek, J. Appl. Crystallogr. 36 (2003) 7.

[39] L.J. Farrugia, J. Appl. Crystallogr. 30 (1997) 565.

[40] L.J. Farrugia, J. Appl. Crystallogr. 32 (1999) 837.
[41] M.J. Frisch, G.W. Trucks, H.B. Schlegel, G.E. Scuseria, M.A. Robb, J.R. Cheeseman, G. Scalmani, V. Barone, B. Mennucci, G.A. Petersson, H. Nakatsuji, M. Caricato, X. Li, H.P. Hratchian, A.F. Izmaylov, J. Bloino, G. Zheng, J.L. Sonnenberg, M. Hada, M. Ehara, K. Toyota, R. Fukuda, J. Hasegawa, M. Ishida, T. Nakajima, Y. Honda, O. Kitao, H. Nakai, T. Vreven, J.A. Montgomery Jr., J.E. Peralta, F. Ogliaro, M. Bearpark, J.J. Heyd, E. Brothers, K.N. Kudin, V.N. Staroverov, R. Kobayashi, J. Normand, K. Raghavachari, A. Rendell, J.C. Burant, S.S. Iyengar, J. Tomasi, M. Cossi, N. Rega, J.M. Millam, M. Klene, J.E. Knox, J.B. Cross, V. Bakken, C. Adamo, J. Jaramillo, R. Gomperts, R.E. Stratmann, O. Yazyev, A.J. Austin, R. Cammi, C. Pomelli, J.W. Ochterski, R.L. Martin, K. Morokuma, V.G. Zakrzewski, G.A. Voth, P. Salvador, J.J. Dannenberg, S. Dapprich, A.D. Daniels, Ö. Farkas, J.B. Foresman, J.V. Ortiz, J. Cioslowski, D.J. Fox, Gaussian 09, Revision C.01, Gaussian Inc., Wallingford, CT, 2009.
[42] A.D. Becke, J. Chem. Phys. 98 (1993) 5648.
[43] C. Lee, W. Yang, R.G. Parr, Phys. Rev. Sect. B 37 (1988) 785.
[44] (a) A.A. Nagel, D.R. Liston, S. Jung, M. Maher, L.A. Vincent, D. Chapin, Y.L. Chen, S. Hubbard, J.L. Ives, S.B. Jones, J. Med. Chem. 38 (1995) 1084;
(b) M.R. Deluca, S.M. Kerwin, Tetrahedron Lett. 38 (1997) 199;
(c) O. Temiz, I. Oren, E. Sener, I. Yalcin, N. Ucarturk, Farmaco 53 (1998) 337;
(d) S. Sato, S.T. Kajiura, M. Noguchi, K. Takehana, T. Kobayashi, T.J. Tsuji, Antibiot 54 (2001) 102.
[45] E. Oksuzoglu, O. Temiz-Arpaci, B. Tekiner-Gulbas, H. Eroglu, G. Sen, S. Alper, I. Yildiz, N. Diril, E. Aki-Sener, I. Yalcin, Med. Chem. Res. 16 (2007) 1.
[46] M.R. Deluca, S.M. Kerwin, Tetrahedron Lett. 38 (1997) 199.
[47] P.D. Edwards, E.F. Meyer, J. Vijayalakshmi, P.A. Tuthill, D.A. Andisik, B. Gomes, A. Strimpler, J. Am. Chem. Soc. 114 (1992) 1854.
[48] Y. Sato, M. Yamada, S. Yoshida, T. Soneda, M. Ishikawa, T. Nizato, K. Suzuki, F.J. Konno, Med. Chem. 41 (1998) 3015.
[49] A.D. Rodriguez, C. Ramrez, I.I. Rodiguez, E. Gonzalez, Org. Lett. 1 (1999) 527.
[50] W. Sun, W. Li, J. Li, J. Zhang, L. Du, M. Li, Tetrahedron Lett. 53 (2012) 2332.
[51] L. Turker, E. Sener, I. Yalcin, U. Akbulut, I. Kayalidere, Sci. Pharm. 58 (1990) 107.
[52] R.S. Varma, D.J. Kumar, Heterocycl. Chem. 351 (1998) 539.
[53] K.H. Park, K. Jun, S.R. Shin, S.W. Oh, Tetrahedron Lett. 37 (1996) 8869.
[54] R.G. Srivastava, P.S. Venkataramani, Synth. Commun. 18 (1988) 1537.
[55] G.J. Speier, Mol. Catal. 41 (1987) 253.
[56] Y. Riadi, R. Mamouni, R. Azzalou, M. E.Haddad, S. Routier, G. Guillaumet, S. Laza, Tetrahedron Lett. 52 (2011) 3492.
[57] B. Maleki, H. Salehabadi, M.K. Moghaddam, Acta Chim. Slov. 57 (2010) 741.
[58] R. Sazaeli, H. Aliyan, Appl. Catal. A Gen. 74 (2009) 353.